Original Article

Trade-off between physical and metallurgical properties of dr iron ore pellets

Jean Philippe Santos Gherardi de Alencar [1*]

Abstract

This study investigates the trade-off between mechanical strength and metallurgical performance in direct reduction (DR) iron ore pellets, a critical challenge in pellet design. A statistically structured experimental design was applied to evaluate the influence of key process parameters - carbon content in green pellets, anthracite particle size, and grate speed - on compressive strength (CCS) and metallization degree (Met). Physical, metallurgical, and microstructural characterizations were conducted, including porosity analysis and optical microscopy. Regression models were developed using ordinary least squares (OLS) to quantify the relationships between process variables and pellet properties. The model for CCS showed moderate predictive power ($R^2 = 0.50$), while the model for Met demonstrated a strong fit ($R^2 = 0.80$), with carbon content and grate speed emerging as statistically significant predictors. These models revealed a clear inverse correlation between CCS and Met, indicating that higher mechanical strength, while beneficial for handling and durability, can hinder gas diffusion and reduce reduction efficiency due to lower porosity and fewer reactive sites. The findings were validated through industrial-scale basket tests in a Midrex reactor, confirming the laboratory trends and reinforcing the importance of data-driven strategies for optimizing pellet performance.

Keywords: Iron ore pellets; Direct reduction; Compressive strength; Metallization.

1 Introduction

Iron ore pellets are vital in the steelmaking industry, serving as a primary feed material for blast furnaces and direct reduction processes [1]. The efficiency of ironmaking production is heavily influenced by the properties of these pellets, which must exhibit a delicate balance between physical strength and metallurgical behavior [2].

The production of iron ore pellets involves optimizing various parameters, including pellet feed composition, fuels and fluxes quality, particle size distribution, and treatment conditions, to achieve desirable properties [3]. The performance of Direct Reduction (DR) Pellet, for instance, is governed by two broad categories of properties: (a) physical/mechanical properties - including cold crushing strength (CCS), tumble index (TI), abrasion resistance and porosity; and (b) metallurgical properties - notably reducibility, degree of metallization (Met), reduction degradation index (RDI), and behavior under high-temperature reduction. An enduring trade-off exists: higher mechanical strength typically correlates with lower internal porosity, impeding gas diffusion essential for efficient reduction [4-6].

Recent research strongly reinforces that this trade-off remains a central issue in contemporary pellet technology. Pal et al. [3] achieved an 8% increase in the reducibility index (RI) by optimizing induration temperature and additive sizing, with some impact on CCS. Meanwhile, Li et al. [7] demonstrated that fine iron filings can improve compressive strength by reducing pellet porosity but may alter metallurgical behavior through microstructural changes. Investigations by Xu et al. [8] into basicity effects revealed a predictable inverse link between porosity and strength—highlighting the familiar strength-versus-permeability dilemma.

Furthermore, as the industry pursues decarbonization, new challenges emerge in hydrogen-based reduction environments. Özgün et al. [9] and Heidari et al. [10] documented how pellet behavior changes during hydrogen reduction—including risk of sticking, swelling, or unexpected brittleness—due to altered diffusion and phase transformations. These studies reiterate the necessity of maintaining a balanced porosity-to-strength ratio, even as reduction atmospheres evolve.

Taken collectively, the literature confirms that the physical versus metallurgical trade-off remains a pressing challenge. The present work aims to quantify this trade-off for DR pellets using a statistically structured experimental design. Our goal was to elucidate how some process variables—such as carbon content, fuel size, and firing conditions—influence the dual demands of mechanical integrity and reduction behavior, thus enabling specification flexibility grounded in data-driven strategies that benefit producers and customers alike.

[1] *Diretoria de Desenvolvimento de Negócios e Produto, VALE SA, Nova Lima, MG, Brasil.*

**Corresponding author: jeanpga@gmail.com*

2 Development

This study aims to develop statistical models that establish correlations between key process parameters (grate speed, carbon content in the green pellet, and coal particle size distribution) and the resulting physical and metallurgical properties of iron ore pellets. In doing so, it also seeks to identify and quantify the trade-offs between these properties as a function of variations in the aforementioned factors, providing a comprehensive understanding of their interdependencies and implications for product optimization.

2.1 Characterization of raw materials used in the project

The pellet feed sample studied was collected from the Vitória pelletizing industrial plant and subsequently characterized at VALE Ferrous Technology Center (CTF). Table 1 and Figure 1 show the global chemical analysis and particle size distribution of the pellet feed.

Similarly, the batch of anthracite used in the tests originated from the Vitória pelletizing plant and is a type commonly supplied to the facility (Table 2). The particle size was deliberately adjusted to obtain three distinct ranges: 50% <325 mesh, 75% <325 mesh, and 100% <325 mesh. The central value of 75% <325 mesh represents the average observed in operations, while 50% and 100% were selected as extremes to assess the impact of this parameter on the process.

2.2 Experimental design

Once the study variables were defined, a test program was developed to generate sufficient results for analyzing the influence of each parameter on output variables and to support the creation of statistical models for pellet properties.

A factorial design with central point replication was implemented. Table 3 lists the experimental points evaluated.

The central values were based on industrial setup references. The lower and upper limits of each parameter were extrapolated to ensure sensitivity in the results while remaining feasible for execution.

Production rate was controlled by adjusting the burning speed (4.48 m/min), which varied by ±7% relative to the central point.

The tests required to evaluate pellet properties included:

- Global chemical analysis
- Compressive Strength (ISO 4700)
- Tumble Index (ISO 3271)

Table 1. Chemical composition of Pellet Feed studied

Sample	Fe (%)	FeO (%)	SiO_2 (%)	Al_2O_3 (%)	MgO (%)	CaO (%)	Mn (%)	LOI (%)	P (%)
DR PF	69.15	-	0.58	0.30	0.02	0.03	0.04	0.92	0.023

Table 2. Anthracite Chemical Composition.

Chemical in Dry Basis (%)			Sample Charac			Ash Chemical Analysis (%)										
Fixed Carbon	Volatile	Ash	C (%)	S (%)	Spec.Heat (cal/g)	Fe_2O_3	SiO_2	Al_2O_3	MgO	CaO	MnO	P_2O_5	TiO_2	Na_2O	K_2O	SO_3
70.5	13.4	16.1	73.6	1.2	6768.57	6.3	46.1	29.8	1.5	4.3	0.4	0.5	1.6	1.8	1.6	4.3

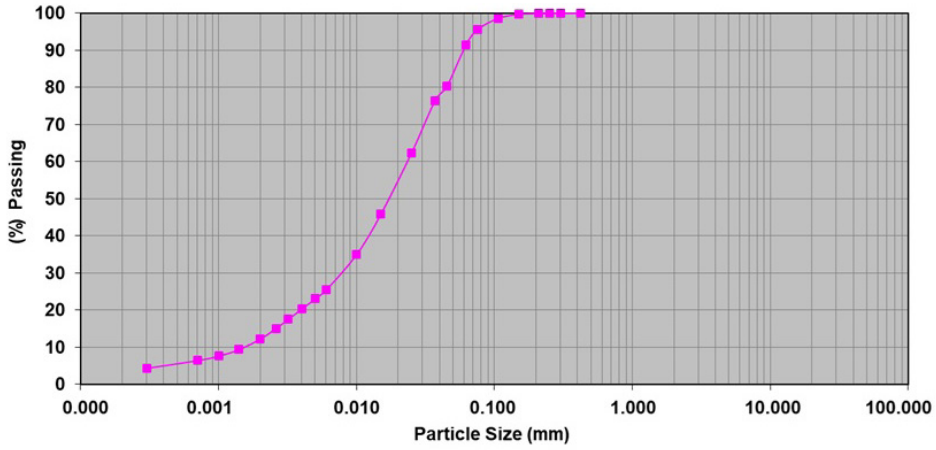

Figure 1. Particle size distribution of DR Pellet Feed studied.

Table 3. Factorial Design of Experiments

Test Number	%C	Anthracite Particle Size	Grate Speed
1	0.6	50% < 325#	High
2	0.6	50% < 325#	Low
3	0.6	100% < 325#	High
4	0.6	100% < 325#	Low
5	1.2	50% < 325#	High
6	1.2	50% < 325#	Low
7	1.2	100% < 325#	High
8	1.2	100% < 325#	Low
Central Point	0.9	75% < 325#	Medium

- Drop Test (internal methodology)

- Dynamic Disintegration (ISO 11257)

The drop test was performed according to an internal methodology developed by VALE, aiming to assess the disintegration resistance of fired pellets under impact conditions. The test consists of dropping a sample of pellets from a standard height of 2.0 meters, repeating the procedure 10 consecutive times. After the drops, the percentage of disintegration is determined by the fraction of material that breaks into particles smaller than 0.5 mm.

Additionally, pellets with compressive strength near the sample average underwent the following characterizations:

- Optical microscopy of cross-sections to quantify phase distribution (area %), total macroporosity, and degree of maturation.

- Mercury porosimetry to assess open porosity in the mesopore range.

Microstructural characterization of the pellets was conducted using fragments collected after the compressive strength test, selecting those with average strength values representative of the sample set. In the cross-section of the embedded specimen, four distinct regions were considered from the outer layer inward: shell, outer mantle, inner mantle, and core (see Figure 2).

The degree of maturation (DM), as defined by the VALE's Materials Characterization Laboratory, refers to the stage of internal microstructural development, encompassing the morphology of hematite grains, the formation of inter and intragranular slag, and the distribution and size of pores. According to the adopted classification, maturation degree is divided into four levels: A, B, C, and D. Level A corresponds to pellets with minimal microstructural evolution, consisting predominantly of hematite while Level D indicates a highly advanced, and sometimes excessive, microstructural transformation.

Total microstructure was assessed by image analysis of polished pellet cross-sections obtained using optical microscopy. The microscope employed for these analyses was a Carl Zeiss Axio Imager Z2m model. An internal software was utilized to segment microstructures regions, based on contrast and morphological criteria. For each sample, at least ten fields were examined, and the microstructure was quantified as the ratio of the area occupied by microstructural features to the total area of the analyzed section.

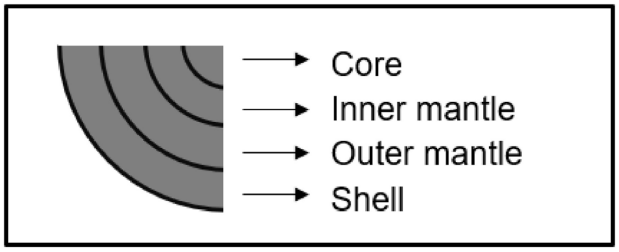

Figure 2. Schematic illustration of pellet sections.

To complement the microstructural analysis, porosity and pore characteristics were evaluated using mercury intrusion porosimeter, a highly effective technique for measuring open porosity within the mesopore and macropore range (30 nm to 360 μm).

These characterizations were conducted to support explanations of how process parameters affect the physical and metallurgical quality of the pellets.

3 Results and discussions

3.1 Chemical analysis results of fired pellets

The chemical analyses of the fired pellets from the experiments are presented in Table 4. The minor variations observed among the chemical analyses do not compromise the study's propositions and are justified by the intrinsic variability of raw materials and the pellet firing process in the pot grate.

The FeO contents in the pellets are low, indicating that there was no over-firing of the samples. These values are typically found in DR pellets produced in Tubarão.

Table 4. Chemical Analysis of All Fired Pellets Produced

Sample	Fe(%)	FeO(%)	SiO_2(%)	Al_2O_3(%)	CaO(%)	MgO(%)	Mn(%)	P(%)	B_2
Pellet 1	67.96	0.10	1.32	0.44	0.74	0.04	0.05	0.027	0.56
Pellet 2	67.97	0.11	1.35	0.44	0.75	0.04	0.05	0.027	0.55
Pellet 3	68.06	0.14	1.25	0.43	0.74	0.03	0.05	0.024	0.59
Pellet 4	67.91	0.11	1.32	0.39	0.74	0.04	0.05	0.027	0.56
Pellet 5	67.72	0.25	1.37	0.46	0.85	0.05	0.05	0.026	0.62
Pellet 6	67.91	0.15	1.35	0.44	0.76	0.04	0.05	0.028	0.56
Pellet 7	67.90	0.21	1.44	0.42	0.74	0.06	0.05	0.028	0.51
Pellet 8	68.03	0.13	1.26	0.46	0.75	0.03	0.05	0.027	0.60
Pellet 9	67.93	0.16	1.34	0.49	0.78	0.03	0.05	0.026	0.58
Pellet 10	67.98	0.21	1.32	0.44	0.77	0.02	0.05	0.027	0.58

Table 5. Physical Analysis of All Fired Pellets Produced

Samples	Green Pellet				Fired Pellet				
	NQ	RCPCU (daN/p)	RCPCS (daN/p)	H_2O (%)	TI +6,3mm (%)	AI -0,5mm (%)	CCS (daN/p)	Drop Test +6,3mm (%)	Drop Test -0,5mm (%)
1	6.4	1.7	8.5	8.3	96.2	3.6	343	99.9	0.0
2	12.3	1.5	5.6	7.0	96.3	3.5	336	99.9	0.0
3	7.5	1.3	7.4	8.0	95.9	3.9	326	99.8	0.0
4	6.9	1.4	8.1	8.6	96.3	3.5	353	99.7	0.1
5	5.6	1.1	6.0	8.2	90.0	9.3	278	99.3	0.4
6	5.5	1.3	6.3	8.5	95.8	3.9	315	99.5	0.3
7	9.1	1.6	6.8	9.0	96.3	3.5	282	99.4	0.4
8	9.0	1.6	7.8	8.4	95.8	3.8	301	99.6	0.2
9	8.8	1.5	8.6	9.0	96.1	3.6	370	99.9	0.0
10	8.9	1.4	7.4	8.8	96.5	3.3	368	99.7	0.1

Where: NQ: number of drops; RCPCU: wet resistance of green pellet; RCPCS: resistance of green pellet after drying; TI: Tumble Index
AI: Abrasion Index

3.2 Physical, metallurgical, and microstructural analysis of fired pellets

Table 5 presents the physical characterization results of the fired pellets. The overall physical quality of both green and fired pellets was very good, with the exception of the abrasion index for sample 5, which was considered anomalous/outlier.

Table 6 shows the metallurgical quality of the fired pellets, including metallization degree (Met) and disintegration index (RDI). The results indicate good metallurgical performance across most samples.

Tables 7 to 9 summarize the results of microstructural characterization via optical microscopy (OM), image-based porosimetry, and mercury intrusion porosimetry (Hg), respectively. These analyses provide insights into phase distribution, porosity by region, and pore structure, supporting the interpretation of how process parameters affect pellet quality.

This classification system categorizes maturation into four distinct levels: A, B, C, and D. Level A denotes pellets with limited microstructural transformation, predominantly composed of hematite. In contrast, Level D signifies a highly advanced, and in some cases excessive, microstructural evolution. Levels B and C represent intermediate stages, characterized by more refined microstructures that contribute to enhanced compressive strength [11].

Table 6. Metallurgical Analysis of All Fired Pellets Produced

Sample	ISO11257	
	- 3,15mm (%)	G.M. (%)
1	0.69	94.76
2	0.92	92.82
3	1.27	95.09
4	0.73	93.65
5	1.89	95.53
6	0.67	94.91
7	0.38	95.27
8	0.14	95.05
9	0.33	94.35
10	0.35	94.85

As shown in the table and as anticipated, the pellets with higher fixed carbon content exhibited greater microstructural evolution. The pellets that approached maturation levels C and D were those with 1.2% fixed carbon under low production rates, as well as those with an intermediate carbon content (0.9%C).

Table 7. Phase quantification and degree of maturation via OM

Sample	Phases Classification (%)				Maturation Degree			
	Silicate	Ferrite	Magnetite	Hematite	Shell	Outer Mantle	Inner Mantle	Core
1	1.9	1.1	0.5	96.5	B	B	B	BC
2	1.7	1.3	0.5	96.5	B	B	BC	BC
3	1.4	0.8	0.2	97.6	B	B	B	B
4	0.8	0.9	0.3	98.1	B	B	BC	BC
5	1.2	0.5	0.1	98.3	B	BC	D	D
6	2.1	0.4	0.1	97.4	C	C	CD	D
7	1.1	0.1	0.0	98.1	BC	BC	D	D
8	1.8	0.9	0.0	97.2	BC	BC	CD	D
9	2.1	0.3	0.3	97.3	BC	BC	C	D
10	0.9	0.4	1.1	97.5	C	C	CD	D

Table 8. Porosity by pellet region as observed via optical microscopy

Sample	Porosity (%)			
	Shell	Outer Mantle	Inner Mantle	Core
1	25.2	26.0	32.0	33.1
2	27.9	30.4	33.7	37.4
3	30.4	33.7	36.1	37.0
4	31.1	32.0	35.3	36.9
5	31.0	32.1	36.4	38.1
6	33.1	36.7	42.2	41.8
7	30.2	31.1	36.9	35.5
8	30.0	30.5	35.4	37.3
9	28.2	31.2	35.4	37.3
10	28.9	30.0	35.3	38.4

Table 9. Porosity of fired pellets measured by mercury intrusion porosimetry

	Porosity(%)	Average Diameter(um)	Total Area (m^2/g)
1	26.61	0.34	0.87
2	25.34	0.37	0.74
3	30.55	0.36	0.97
4	26.41	0.26	1.11
5	27.97	0.45	0.75
6	23.39	0.38	0.69
7	23.36	0.28	1.13
8	22.69	0.31	0.81
9	21.92	0.43	0.57
10	19.53	0.39	0.56

3.3 Statistical models

Ordinary Least Squares (OLS) regression is a fundamental statistical technique used to estimate the relationships between one or more independent variables and a dependent variable. In OLS, the model assumes a linear relationship, and the coefficients are determined by minimizing the sum of the squared differences between the observed values and the values predicted by the model. This approach yields the best linear unbiased estimators under the Gauss–Markov assumptions, provided that the errors are homoscedastic and uncorrelated [12]. This model was chosen due to its robustness in identifying linear relationships between independent variables and dependent variables, and because it is widely used in iron ore pelletization studies [13-16].

To develop the regression models, we applied both simple and multiple linear regression techniques using ordinary least squares (OLS) estimation. The dependent variables—such as CCS, Met, IA, and RDI—were modeled as linear functions of independent predictors including C, Ciclo, and Gran. Attempts were made to include Porosity and Maturation Degree as variables in the model; however, due to multicollinearity effects, they were excluded. For

each model, we computed the coefficient of determination (R^2) to assess the proportion of variance explained by the predictors. Additionally, we conducted hypothesis testing on the regression coefficients using t-tests and reported the associated p-values to evaluate the statistical significance of each predictor.

A p-value below 0.05 was considered indicative of a significant contribution to the model. Residual diagnostics, including histogram and Q-Q plots, were also performed to assess the normality assumption of the residuals, which is critical for the validity of inference in linear regression.

The linear regression model developed for CCS (Equation 1) demonstrated a good fit, as illustrated in Figure 3. However, when examining the statistical significance (p-value) of the predictors, it is evident that predictor C is the most statistically significant.

Equation 1:

$$CCS = 536.7860 + -75.8333 * C + - 30.6838 * Ciclo + -0.0500 * Gran \quad (1)$$

R^2: 0.5006

P-values for CCS:

- const: 0.0117
- C: 0.0651
- Ciclo: 0.3752
- Gran: 0.9055

The regression model obtained for the variable Met, presented in Equation 2, showed an excellent fit, explaining nearly 80% of the model's variability. Predictors C and Ciclo were the most statistically significant contributors to the model.

Equation 2:

$$Met = 85.0629 + 1.8500 * C + 1.6749 * Ciclo + 0.0052 * Gran \quad (2)$$

R^2: 0.7956

P-values for Met:

- const: 0.0000

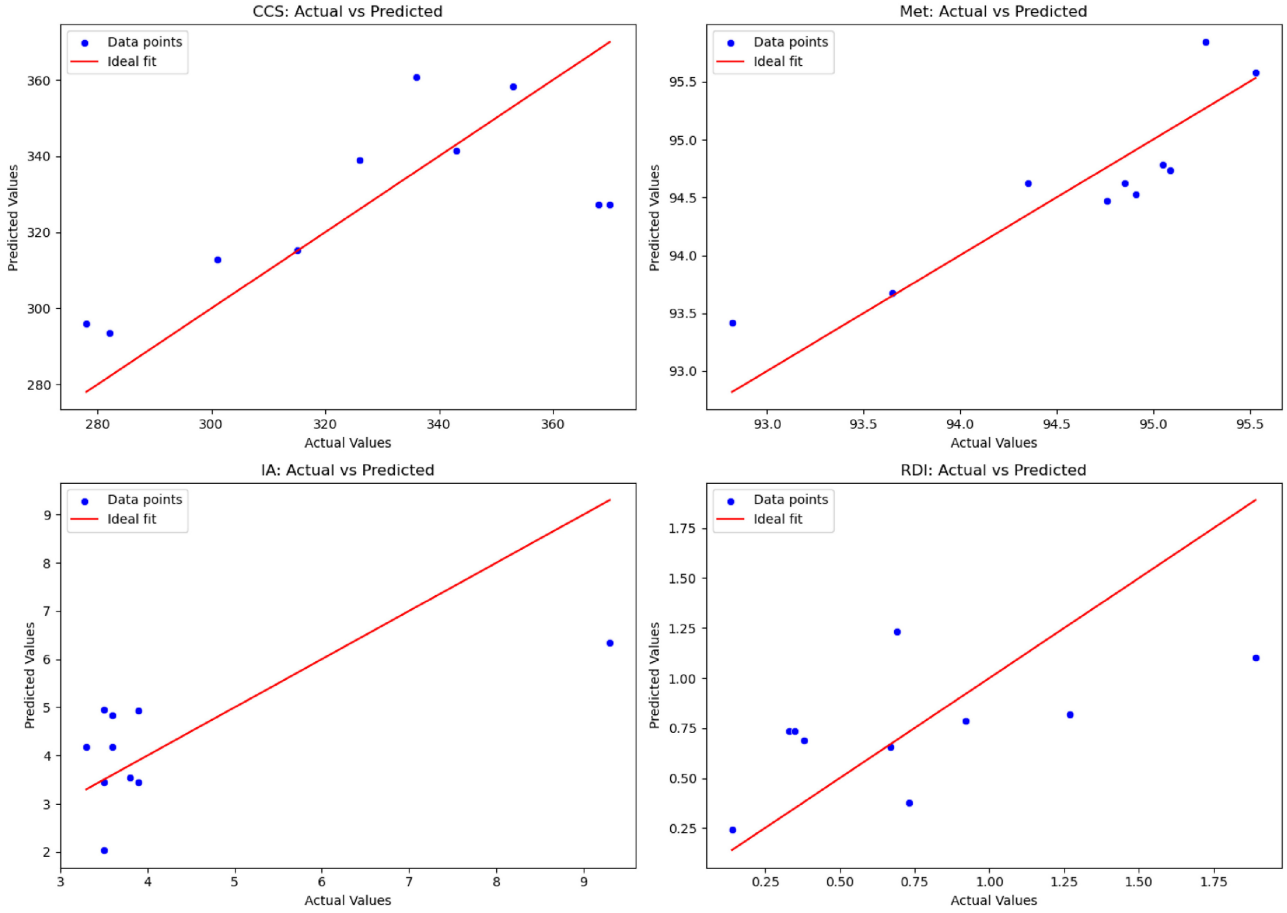

Figure 3. Plot of predicted vs actual values for the dependent variables CCS, Met, IA, and RDI.

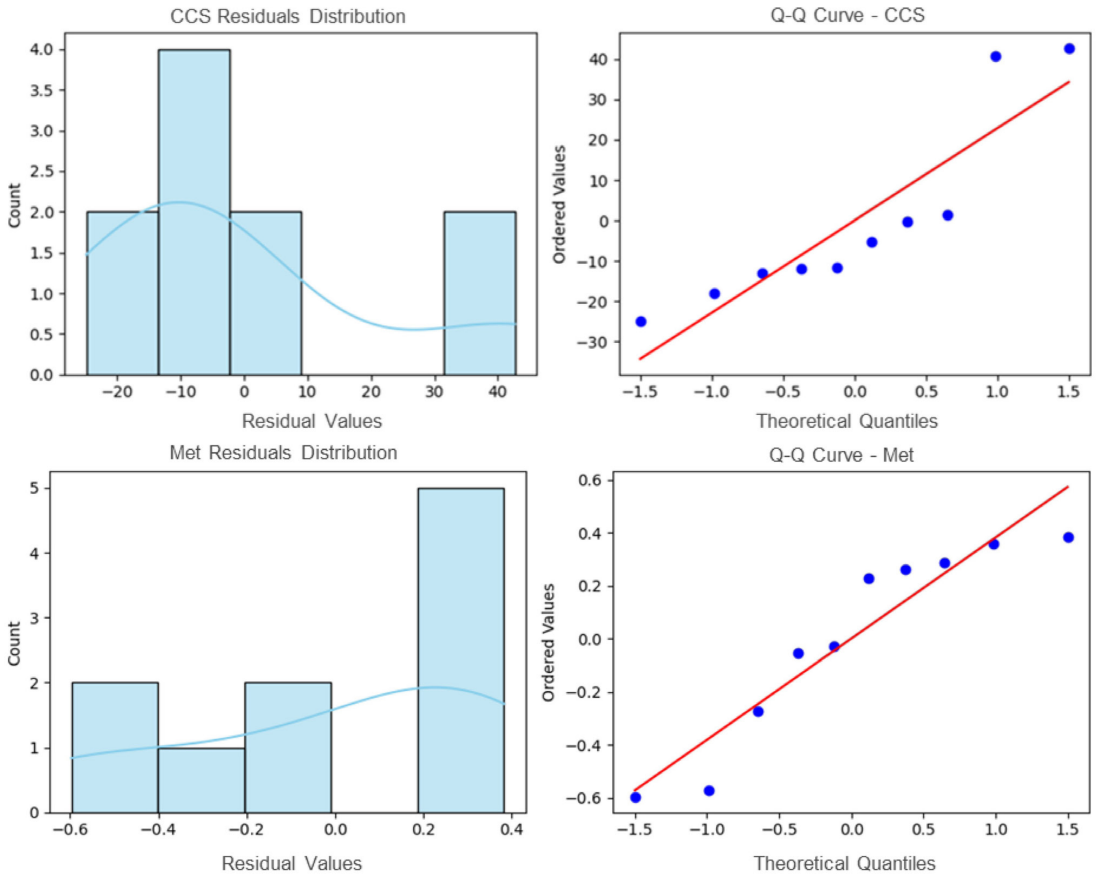

Figure 4. Distribution Histogram and Q-Q Plot of the Residuals for the CCS and Met Models.

- C: 0.0136
- Ciclo: 0.0168
- Gran: 0.4495

On the other hand, the models developed for IA and RDI showed moderate fits (see Figure 3), with R^2 values of 0.42 and 0.31, respectively. Furthermore, neither model includes predictors that are statistically significant at the 5% level. The low explanatory power of these parameters is associated with the fact that they are influenced by other predictive factors that were not mapped and may also be related to the presence of outlier data points (e.g., pellet #5 for IA).

By evaluating the residual distribution of the CCS and Met models through the residual histograms and Q-Q (Quantile-Quantile) plots shown in Figure 4, it is observed that the residuals tend to follow a normal distribution, supporting the validity of the models within the domain of the modeled data.

Since the objective of this study was to quantitatively establish a relationship between the main physical and metallurgical variables and given that the predictor variables are practically the same for both CCS and Met, a direct correlation between them was pursued. However, considering the distinct behavior observed in the physical tests of Pellet #5 and acknowledging that, in industrial settings, the C values typically range from 0.9% to 1.2%, it was decided to exclude the data points where C was equal to 0.6% from the correlation analysis between Met and CCS. As shown in Figure 5, this correlation proved to be strong and inversely proportional, as expected.

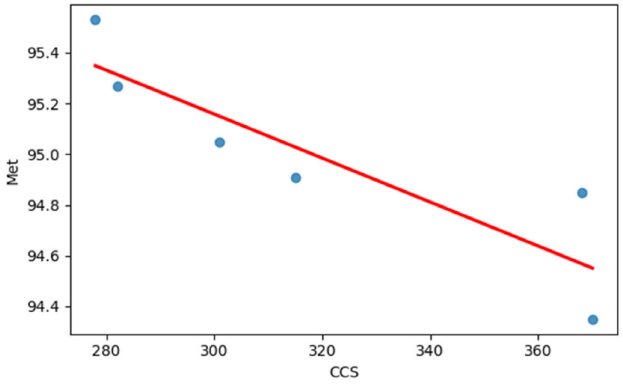

Figure 5. Correlation between Met and CCS excluding C=0.6%.

After excluding the data points where C = 0.6%, Equation 3 shows that for each additional unit in CCS, a

reduction of approximately 0.0087 units in Met is expected. The R^2 value of 0.7797 indicates that about 78.0% of the variation in Met can be explained by CCS.

Equation 3:

$$\text{Met} = 97.7591 + (-0.0087) \times \text{CCS} \quad (3)$$

$$R^2: 0.7797$$

3.4 Industrial scale validation

In order to deepen the understanding and validate the quantitative dilemma observed in the laboratory, two pellet samples (#7 and #9) were sent to a Direct Reduction reactor operator. These corresponded to the following conditions: Pellet #7 (1.2% C, 100% <325# and 4.82 m/min) and Pellet #9 (0.9% C, 75% <325# and 4.18 m/min). Pellet #7 exhibited the lowest compressive strength, whereas pellet #9 showed the highest compressive strength.

This industrial test was conducted in a Midrex reactor using the basket test methodology. Essentially, 10 split metallic baskets were prepared and simultaneously loaded with equal quantities of pellets #7 and #9. All baskets were collected during a single shift of approximately 6 hours and subsequently subjected to metallization analysis.

Table 10 presents the comparative results of these pellets in both laboratory and industrial tests. It can be observed that the metallization trends identified in the laboratory were confirmed, with pellet A achieving the highest metallization. According to the statistical models, the 88 daN difference in compressive strength between these pellets would correspond to a metallization gain of approximately 0.76%, whereas the actual average gain observed in the basket tests was 0.54%.

The standard deviations for the basket test metallization were 0.32% for pellet #7 and 0.38% for pellet #9, based on ten baskets per sample. Despite these levels of variability, the observed difference in mean metallization between the two samples (0.54%) remained statistically significant (Welch's t-test, two-sided: $t = 3.44$, $df \approx 18$, $p < 0.01$). Therefore, this industrial trend supports the understanding that pellets produced from the same feedstock and under controlled conditions may exhibit a trade-off between metallurgical and physical properties, such as compressive strength and metallization.

The regressions models developed in this study and the basket test, a negative correlation was observed between CCS and the metallization rate (Met).

This phenomenon can be attributed to several microstructural factors:

- Higher CCS is typically associated with increased pellet density and reduced porosity, which can hinder the diffusion of reducing gases such as H_2 and CO during the reduction process. This limitation in gas permeability slows down the reduction kinetics, thereby lowering the metallization rate.

- A more compact internal structure restricts the available surface area and reactive sites for the reduction of iron oxides, further impeding the overall reactivity of the pellet.

These findings are consistent with previous studies. For instance, Xu et al.[8] demonstrated that pellets with lower porosity exhibit higher compressive strength but reduced reducibility, due to limited gas diffusion pathways and fewer internal reaction sites. Bersenev et al. [17] analyzed the evolution of porosity in iron ore pellets roughout their lifecycle—from green pellets to fully reduced states. They found that reduction increases porosity significantly (by 100–200%), which enhances gas diffusion and metallization. Conversely, pellets with initially low porosity (and thus higher CCS) tend to exhibit lower reducibility due to restricted gas pathways.

On the other hand, Giesche [18] discussed the interdependence of surface area, density, and porosity in powders, noting that higher density (and thus lower porosity) materials often exhibit greater mechanical strength but reduced reactivity, a principle that applies directly to iron ore pellet behavior during reduction.

4 Conclusions

This study successfully quantified the trade-off between compressive strength (CCS) and metallization degree (Met) in direct reduction (DR) iron ore pellets, using a statistically structured experimental design. By systematically varying key process parameters—namely carbon content in the green pellet, anthracite particle size, and grate speed—we were able to develop regression models that describe how these variables influence both the physical and metallurgical performance of fired pellets.

The results revealed a clear and statistically significant inverse relationship between CCS and Met. Higher CCS values, while beneficial for mechanical handling and resistance to

Table 10. Consolidated results of Pellet #7 and #9

Pellet	CCS (daN)	ISO-Lab	Met (%)	ISO-Lab	Met (%)	Basket Test
#7	282		95.27		94.91	
#9	370		94.35		94.37	
Dif	-88		0.92		0.54	

degradation during transportation and reactor loading, were consistently associated with lower metallization rates. This behavior is attributed to microstructural changes: increased CCS correlates with higher pellet density and reduced porosity, which in turn restricts the diffusion of reducing gases such as H_2 and CO. This limitation impairs the kinetics of the reduction reactions, leading to lower degrees of metallization. Optical microscopy and mercury porosimetry confirmed that pellets with higher CCS exhibited more compact internal structures and lower open porosity, reducing the number of reactive sites available for gas-solid interactions.

The regression models developed in this study demonstrated good predictive power, particularly for CCS and Met, with R^2 values of 0.50 and 0.80, respectively. These models not only provide a quantitative understanding of the trade-off but also offer a practical tool for process optimization. For instance, the model suggests that a reduction of 88 daN in CCS could yield an increase of approximately 0.76% in Met—an insight that can guide operational decisions depending on whether mechanical robustness or metallurgical performance is prioritized.

Importantly, the laboratory findings were validated through industrial-scale basket tests conducted in a Midrex reactor. The observed trends in metallization mirrored those predicted by the models, reinforcing the reliability of the experimental approach and the practical relevance of the results. This validation step is crucial, as it bridges the gap between controlled laboratory conditions and the complexities of real-world operations.

Ultimately, this work contributes to a deeper understanding of the physical-metallurgical trade-off in pellet design and provides a data-driven foundation for tailoring pellet properties to specific operational needs. Future research could expand on these findings by incorporating additional variables such as flux composition, pellet size distribution, and alternative binders, as well as exploring non-linear modeling techniques to capture more complex interactions.

References

1 Shin SG, Kim WH, Min DJ. A study on the effect of alumina on the morphology and reduction behavior of sinter by in situ observation. Metals. 2021;11(5):740. https://doi.org/10.3390/met11050740.

2 Hao Q, Liu W, Gao W, Wang X. A multi-scale fusion convolutional network for time-series silicon prediction in blast furnaces. Mathematics. 2025;13(8):1347. https://doi.org/10.3390/math13081347.

3 Pal J, Ghorai S, Goswami MC, Ghosh S, Ghosh D, Bandyopadhyay D. Development of fluxed iron oxide pellets strengthened by CO_2 treatment for use in basic oxygen steel making. ISIJ International. 2009;49(2):210-219. https://doi.org/10.2355/isijinternational.49.210.

4 Meyer K. Pelletizing of iron ores. Berlin: Springer-Verlag; 1980. 302 p.

5 Hegde, V. S., Kong, L. T., Paquet, G., & Lu, W. K. Fluxed pellets with high coke breeze additions. In: Ironmaking Conference Proceedings; 1990. Warrendale, PA. Warrendale: Association of Iron & Steel Engineers; 1990. p. 3-11.

6 Paquet G, Gourde S. Physical tests: their meaning and relevance to iron pellets. In: AISTech 2005 Proceedings; 2005; Warrendale, PA. Warrendale: Association of Iron & Steel Engineers; 2005. COREM Technical Article.

7 Li Y, Zhang H, Wang J, Liu X. Influence of fine iron filings on porosity and compressive strength of iron ore pellets. Journal of Iron and Steel Research International. 2022;29(11):1023-1031.

8 Xu G, Liu Y, Zhao F, Wang Y. Effect of basicity on porosity and strength of iron ore pellets. Steel in Translation. 2023;53(12):1137-1143. https://doi.org/10.3103/S096709122370002X.

9 Özgün Ö, Dirba I, Gutfleisch O, Ma Y, Raabe D. Green ironmaking at higher H_2 pressure: Reduction kinetics and microstructure formation during hydrogen-based direct reduction of hematite pellets. Journal of Sustainable Metallurgy. 2024;10(3):1127-1140. https://doi.org/10.1007/s40831-024-00877-4. PMid:39280577.

10 Heidari M, Zakeri A, Coley K, Tafaghodi L. Hydrogen-based direct reduction of industrial iron ore pellets: Thermogravimetric and microstructural studies. In: Metallurgy and Materials Society of CIM, editor. Proceedings of the 63rd Conf. Metallurgists (COM 2024); 2024; Cham. Cham: Springer; 2024. p. 1755-1661. https://doi.org/10.1007/978-3-031-67398-6_284.

11 Mafra WL, Resende VG, Vieira MBH, Domingues ALL. Basicidade binária como parâmetro de qualidade no desenvolvimento de pelotas tipo alto-forno. In: Anais do 1º Simpósio Brasileiro de Aglomeração de Minério de Ferro; 2014 set 1-4; Belo Horizonte, MG, Brazil. São Paulo: ABM Proceedings; 2014.

12 Hansen BE. A modern gauss–markov theorem. Econometrica. 2022;90(3):1283-1294. https://doi.org/10.3982/ECTA19255.

13 Mo W, Feng Y, Wang Z, Yang J, Feng J, Su X. Optimization of the evaluation method for bentonite used in iron ore pelletizing. Metallurgical and Materials Transactions. B, Process Metallurgy and Materials Processing Science. 2024;55(5):3464-3477. https://doi.org/10.1007/s11663-024-03187-y.

14 Majumder S, Desai VJ, Arunprasath J, Runkana V, Prasad AS, Ravindranath M, et al. Model-based On-line Optimization of Iron Ore Pellet Induration on a Moving Grate Furnace. In: International Mineral Processing Congress; 2022; New Delhi. New Delhi; 2022 [cited 2025 Sep 24]. Available at: https://www.researchgate.net/publication/373069410_MODEL-BASED_ON-LINE_OPTIMIZATION_OF_IRON_ORE_PELLET_INDURATION_ON_A_MOVING_GRATE_FURNACE

15 Ngo Quoc Dung N, Tran Xuan Hai T, Nguyen Minh Thuyet N, Nguyen Quang Tung NQ, Barsiwal A, Nguyen Hoang Viet NH. Enhanced compressive strength of fired iron ore pellets: effects of blending fine and coarse particle concentrates. Journal of Powder Materials. 2025;32(4):315-329. https://doi.org/10.4150/jpm.2025.00129.

16 Gao Q, Zhang Y, Jiang X, Zheng H, Shen F. Prediction model of iron ore pellet ambient strength and sensitivity analysis on the influence factors. Metals. 2018;8(8):593. https://doi.org/10.3390/met8080593.

17 Bersenev IS, Vokhmyakova IS, Ozornin NK, Pokolenko SI, Sabirov ER, Spirin NA. Porosity of iron-ore pellets at different stages of roasting and reduction. Steel in Translation. 2023;53(12):8-13. https://doi.org/10.3103/S096709122370002X.

18 Giesche H. Mercury porosimetry: a general (practical) overview. Particle & Particle Systems Characterization. 2000;17(3):116-122.

Received: 24 Sep 2025
Accepted: 2 Dec 2025

Editor-in-charge:
André Luiz Vasconcellos da Costa e Silva